HHS Public Access

Author manuscript

J Appl Toxicol. Author manuscript; available in PMC 2015 November 01.

Published in final edited form as:

J Appl Toxicol. 2014 November ; 34(11): 1188–1199. doi:10.1002/jat.3018.

Single-walled carbon nanotube and graphene nanodelivery of gambogic acid increases its cytotoxicity in breast and pancreatic cancer cells

Lamya M Saeed[a], **Meena Mahmood**[a], **Sebastian J. Pyrek**[b], **Tariq Fahmi**[b], **Yang Xu**[a], **Thikra Mustafa**[a,d], **Zeid A. Nima**[a], **Stacie M. Bratton**[b], **Dan Casciano**[a], **Enkeleda Dervishi**[a,c], **Anna Radominska-Pandya**[b,*], and **Alexandru S. Biris**[a,*]

[a]Center for Integrative Nanotechnology Sciences, University of Arkansas at Little Rock, AR 72204, USA

[b]Department of Biochemistry and Molecular Biology in the College of Medicine at the University of Arkansas for Medical Sciences, Little Rock, AR 72205, USA

[c]Center for Integrated Nanotechnologies, Materials Physics and Application Division, Los Alamos National Laboratory, Los Alamos, NM 87544, USA

[d]Department for Biology, College of Science for Women, University of Baghdad, Baghdad, Iraq

Abstract

Graphene and single-walled carbon nanotubes were used to deliver the natural low-toxicity drug gambogic acid (GA) to breast and pancreatic cancer cells *in vitro*, and the effectiveness of this complex in suppressing cellular integrity was assessed. Cytotoxicity was assessed by measuring lactate dehydrogenase release, mitochondria dehydrogenase activity, mitochondrial membrane depolarization, DNA fragmentation, intracellular lipid content, and membrane permeability/caspase activity. The nanomaterials showed no toxicity at the concentrations used, and the antiproliferative effects of GA were significantly enhanced by nanodelivery. The results suggest that these complexes inhibit human breast and pancreatic cancer cells grown *in vitro*. This analysis represents a first step toward assessing their effectiveness in more complex, targeted, nanodelivery systems.

Keywords

Cancer nanotechnology; Gambogic Acid; Graphene; Single-Walled Carbon Nanotubes; Nanodelivery; Breast cancer; Pancreatic cancer

[*]Correspondence to: Alexandru S. Biris, Center for Integrative Nanotechnology Sciences, University of Arkansas at Little Rock, AR 72204, USA. asbiris@ualr.edu; Anna Radominska-Pandya, Department of Biochemistry and Molecular Biology in the College of Medicine at the University of Arkansas for Medical Sciences, Little Rock, AR 72205, USA. radominskaanna@uams.edu.

Conflict of Interest

The Authors did not report any conflict of interest.

Introduction

Cancer is one of the largest public health concerns in the United States and across the world (Jemal *et al*., 2011; Siegel *et al*., 2013). Breast cancer consistently ranks highest in incidence and death for women globally (Jemal *et al*., 2011), and more than 1 million new cases occur worldwide each year, leading to the deaths of more than 450 000 women annually (Jemal *et al*., 2011). Although survival rates for patients with breast cancer are high compared to those for other types of cancer (Siegel *et al*., 2013), there is still a need for innovative new therapies, especially for patients diagnosed with metastatic cancer.

Pancreatic cancer is another malignancy that continues to pose a significant challenge to physicians and researchers with an incidence to mortality ratio approaching 1 (Jemal *et al*., 2011; Siegel *et al.*, 2013). In the United States, it represents the fourth major reason of cancer death for both men and women (Siegel *et al*., 2013). The 5-year survival rate for localized cancers is only 23%, and that number drops to 6% when regional and distant forms are considered (Siegel *et al*., 2013). Worldwide, pancreatic cancer represents the eighth and ninth leading causes of cancer death in males and females, respectively (Jemal *et al*., 2011). The current treatment options for pancreatic cancer are similar to those for other forms of cancer (i.e., surgery, radiation, and chemotherapy) but seldom lead to a cure and cause many serious side-effects. The poor prognosis for pancreatic cancer is due in part to late diagnosis and extensive metastasis; however, it is also due to poor response to therapeutics (Safioleas and Moulakakis, 2004), caused in part by the extremely dense desmoplasia, which can prevent standard drugs from penetrating the tumor (Tod *et al*., 2013). Therefore, there is a great need for new drugs and better methods of drug delivery.

Here, we have assessed the anticancer properties of a natural, low-toxicity drug, gambogic acid (GA), in breast (MCF-7) and pancreatic (Panc-1) cancer cells. GA is the major active component of gamboge, the golden resin isolated from the plant *Garcinia hanburyi* that has been used in traditional Eastern medicine (Chantarasriwong *et al.*, 2010; Efferth *et al.*, 2007). Recent studies have shown that GA can reduce the growth rate of many kinds of tumor cells such as leukemia (Wang LL *et al.*, 2008), gastric cancer (Yu *et al.*, 2006), hepatoma (Guo *et al.*, 2004), lung carcinoma (Wu *et al.*, 2004), breast carcinoma (Qi *et al.*, 2008), and pancreatic cancer (Wang C *et al*., 2011, 2012) cells.

One of the limitations on the use of GA as a drug is its poor solubility (He *et al.*, 2012) and inadequate oral bioavailability (Zhang *et al*., 2013). Nanodelivery of drugs can improve their water solubility, enhance cellular uptake, and increase formulation stability and shelf life (De Jong and Borm, 2008). Different types of nanosized drug carriers have been described in the literature for the delivery of GA, such as micelles (Qu *et al.* 2009; Saxena and Hussain, 2012; Yu *et al.*, 2013; Zhu *et al.*, 2008) and superparamagnetic iron oxide nanoparticles (Chen *et al.*, 2009; Fang *et al.*, 2012; Liang *et al.*, 2010; Wang C *et al*., 2011). The novelty of this work lies in the use of carbon-based nanomaterials, which we have shown to have potential for use in various biomedical applications (Biris *et al.*, 2011; Karmakar *et al.*, 2011; Mahmood *et al.*, 2012). In this work, we have elected to evaluate two carbon nanomaterials, graphene (Gn) and single-walled carbon nanotubes (SWCNT), as potential carriers for GA.

Gn is an atom-thick carbon monolayer of sp2-bonded carbon atoms arranged in a two-dimensional honeycomb crystal lattice—which is the essential building block of other graphitic materials, such as fullerenes (spherical structure), SWCNT (one-dimensional tubular structure) and graphite (three-dimensional layered structure)—that is of great interest to scientists because of its unique physical and chemical properties (Geim and Novoselov, 2007; Iijima, 1991; Novoselov *et al.*, 2004; Zhang *et al.*, 2012). It has also been demonstrated that simple physisorption via π–π stacking can be employed to load drugs onto these carbon nanomaterials (Sun *et al.*, 2008), which makes them a very desirable material for drug delivery. In addition, owing to the two-dimensional nature of Gn, both sides are available for drug binding (Liu *et al.*, 2008), and therefore provides a large specific surface area for attachment despite its small size.

Gn and SWCNT can also be functionalized with various biomolecules. This allows the design of specialized drug delivery systems, which have been shown to modulate pharmacodynamics/pharmacokinetics and increase efficacy (Sundar and Prajapati, 2012). The presence of oxygen-rich functional groups on the surfaces of Gn oxide and of SWCNT provides enhanced biocompatibility, stability, and solubility in physiological solutions.

The majority of existing studies have reported that Gn sheets cause only minor cytotoxicity in cell lines from various sources (Chang *et al.*, 2011; Lee *et al.*, 2012; Mahmood *et al.*, 2013; Wang K *et al*., 2011; Zhang L. *et al*., 2010; Zhang Y. *et al*., 2010). Specifically, Gn oxides with a dose of less than 20 μg ml^{-1} did not demonstrate any toxicity in the human fibroblast cell line, HDF, and in the same study Gn oxides at either 0.1 or 0.25 mg per animal did not show obvious toxicity to mice (Wang K *et al*., 2011). It has also been reported that (10 or 20 μg ml^{-1}) of SWCNT did not have significant toxic effect on MLO-Y4, HeLa, or Panc-1 cells when incubated for 24 h (Mahmood *et al*., 2009).

The aim of this study was to assess the cytotoxicity of GA in MCF-7 and Panc-1 cancer cells and to determine what effect nanodelivery by either Gn or SWCNT had on the efficacy of this promising, nontoxic, naturally derived drug. We have investigated the cytotoxicity in these cells by measuring lactate dehydrogenase (LDH) release, mitochondrial metabolic activity (WST-1 assay), mitochondrial membrane depolarization, and DNA fragmentation. Change in the intracellular lipid droplet biogenesis in response to GA and its nanodelivery were detected using Nile Red Stain. We have also examined membrane permeability and caspase activity using flow cytometry. Such delivery of GA by either Gn or SWCNT represents a first step toward assessing their effectiveness in more complex, targeted nanodelivery in *in vivo* settings and signals their potential applications in pharmacological and medical fields.

Materials and Methods

Main Reagents

GA (G1000) was purchased from Gaia Chemical Corporation (New Milford, CT, USA). Panc-1 and MCF-7 cells were purchased from ATCC Collection, Inc. (Manassas, VA, USA), and maintained in Dulbecco's modified Eagle's medium from the same company. SWCNTs (82490) were purchased from Sigma-Aldrich (St. Louis, MO, USA). Ethyl alcohol

(95%) was purchased from Fisher Scientific (Pittsburg, PA, USA). Unless differently mentioned, all other reagents and chemicals were of reagent grade and purchased from Sigma-Aldrich.

Nanostructural Materials Preparation

Gn structures were synthesized on Fe/Mo/MgO (1 : 0.1 : 110 molar ratio). The catalyst system was prepared as previously reported (Dervishi *et al.*, 2012). The graphitic nanomaterials were synthesized using an RF generator in an argon methane environment. The as-produced Gn nanostructures were purified with hydrochloric acid. For better dispersion in an aqueous solution, the nanosized, few-layer thick Gn samples were functionalized with carboxylic functional groups (Kim and Kim, 2010). Each solution was continuously washed with distilled water and finally dried in an oven at 100 °C for 12 h.

Preparation of Gambogic Acid-Loaded Graphene and Single-Walled Carbon Nanotubes

Gn and SWCNT (10 μg ml^{-1}) were mixed with GA (0.5, 0.75 and 1μg ml^{-1}) to be described as GA + Gn and GA + SWCNT. First, the samples were vortexed at a high speed for at least 4 h to allow the drug to bind to the nanomaterials *via* π–π stacking (Xu *et al.*, 2012). The samples were then centrifuged and washed three times with distilled water to remove the unbound drug. The loading concentrations of the GA on Gn and SWCNT were determined by UV-Vis absorbance at 360nm measured using a Shimadzu UV-3600 spectrophotometer (Shimadzu Scientific Instruments, Colombia, ME, USA).

Transmission Electron Microscopy Analysis of Nanomaterials

As size and diameter play critical roles in regulating a nanoparticle's internalization and interaction within cells (Liu *et al.*, 2011), transmission electron microscopy (TEM) was used to determine the exact dimensions of the Gn sheets and SWCNT. TEM micrographs were made using the JEOL field-emission JEM-2100 F instrument (JEOL Peabody, Massachusetts, USA). The nanomaterial samples were separately dissolved in isopropanol and sonicated for 30 min to form a homogeneous solution. Next, a few drops of the suspension were deposited on a holey carbon-coated TEM grid for analysis. Selected area diffraction patterns were collected by placing an aperture on the desired area of the TEM micrographs (Dervishi *et al.*, 2012).

Cell Culture and Treatment Conditions

MCF-7 and Panc-1 cells were plated in 75 cm^2 tissue culture flasks at a density of 10^6 cells per dish and maintained in Dulbecco's modified Eagle medium supplemented with 10% fetal bovine serum and 1% penicillin + streptomycin and incubated at 37 °C in a 5% CO_2 humidified incubator. Once the cells were confluent, they were EDTA trypsinized for further experiments.

For experiments where cells were treated with Gn, SWCNT, GA + Gn, or GA + SWCNT, nanomaterials were dispersed into growth medium at a maximum particle concentration of 10 μg ml^{-1} and tip-sonicated for 1 h. The cell growth medium used for plating was then replaced with this treatment medium, and cells were incubated in the treatment media for 24 or 48 h. Fresh treatment media were prepared before each cell treatment.

Transmission Electron Microscopy Analysis of Treated Cells

To verify that both types of nanomaterials were taken up by the cells, additional TEM was performed on cells cultured with SWCNT and nano-Gn sheets at a concentration of 10 μg ml^{-1} for 24 h. A control sample was also processed. Samples were fixed in 3% glutaraldehyde fixative in 0.1 M phosphate buffer, pH 7.2 overnight at 4 °C. After fixation, all of the samples were thoroughly rinsed with a 0.1 M phosphate buffer (pH 7.2), post-fixed in 2% osmium tetroxide in 0.1 M phosphate buffer for 2 h, rinsed in distilled water, and dehydrated in an ethanol solution. The resulting dried specimens were embedded in Spurr's resin, which was polymerized at 70 °C for 15 h. A thickness of 60–100 nm) was generated for light microscopy and TEM analysis. Thin sections mounted on 200 mesh copper grids were stained with uranyl acetate and lead citrate for TEM.

Nanomaterial Toxicity Determination

To determine which concentration of nanomaterials was most suitable for use in future experiments, a concentration-dependent cell membrane integrity assay was performed with both cell lines. MCF-7 and Panc-1 cells were treated with increasing concentrations of Gn or SWCNT, and LDH release was measured at three time points up to 72 h using the LDH assay kit (Cayman Chemical Company, Ann Arbor, MI, USA). Briefly, MCF-7 and Panc-1 cells were seeded on to 96-well plates (25×10^3 per well) and allowed to grow for 24 h before treatment with increasing concentrations (5, 10, 20, 50 μg ml^{-1}) of Gn and SWCNT. After 24, 48, and 72 h, a portion of the supernatant (100 μl) was transferred to new 96-well plates. The plates were incubated for 30 min at room temperature on an orbital shaker. A colorimetric absorbance was recorded at 490 nm with a reference wavelength of 520 nm using a microplate reader for colorimetric detection (BioTek, Winooski, VT, USA). Each experiment was performed in triplicate. Cytotoxicity is expressed relative to the basal LDH release by untreated control cells and presented as mean ± standard error of mean.

Inhibition of MCF-7 and Panc-1 Cell Viability by Gambogic Acid, Gambogic Acid + Graphene, and Gambogic Acid + Single-Walled Carbon Nanotubes

Mitochondrial metabolic activity of MCF-7 and Panc-1 cells after administration of GA, GA + Gn and GA + SWCNT was determined using the WST-1 Cell Proliferation Assay Kit (Cayman Chemical Company, Ann Arbor, MI, USA). This assay takes advantage of the color shift that occurs after mitochondrial dehydrogenase cleaves the tetrazolium salt, WST-1, to formazan in viable cells. Briefly, MCF-7 and Panc-1 cells were seeded on to 96-well plates at a density of 25×10^3 cells per well and allowed to grow for 24 h before treatment with increasing concentrations of GA (0–1 μg ml^{-1}) at a constant Gn or SWCNT concentration (10 μg ml^{-1}). After 48 h incubation, 10 μl of reconstituted WST-1 mixture were added to each well and incubated for 2 h in the dark at 37 °C. The absorbance at 450 nm was measured using a microplate reader (Biotek, Winooski, VT, USA). Wells containing only medium and WST-1 reagent were measured as a background control. All conditions were run in triplicate for statistical analysis. IC_{50} values (the concentration of the drug that inhibits cell viability by 50%) were calculated based on the results of the WST-1 assay.

Determination of Mitochondrial Membrane Potential

The effects of GA, Gn, SWCNT, GA + SWCNT, and GA + Gn on mitochondrial membrane potential (ΔΨm) in MCF-7 and Panc-1 cells were measured using the mitochondrion-specific lipophilic cationic probe, fluorochrome JC-1 (5′,6,6′-tetrachloro-1,1′,3,3′-tetraethylbenzimidazolylcarbocyanine iodide; Sigma-Aldrich) (Fig. 6). MCF-7 and Panc-1 cells were incubated with GA (1 μg ml^{-1}), Gn (10 μg ml^{-1}), SWCNT (10 μg ml^{-1}), GA + Gn (1 + 10 μg ml^{-1}), and GA + SWCNT (0.9 + 10 μg ml^{-1}) for 24 h. After treatment, the cells were incubated with JC-1 dye for 20 min, washed with phosphate-buffered saline, and then visualized under fluorescence microscopy.

Cellular Death Studies Performed by Flow Cytometry

Quantification of the apoptotic cells was done using an Annexin-V-fluorescein isothiocyanate Apoptosis Detection Kit (Biovision, Milpitas, CA, USA) and following the manufacturer's instructions. MCF-7 and Panc-1 cells were incubated in a medium containing increasing concentrations of GA (0–1 μg ml^{-1}) at a constant Gn or SWCNT concentration (10 μg ml^{-1}) at 37 °C for 24 and 48 h. The normal growth medium and 10 μg ml^{-1} (equal to the maximum amount of nanoparticle used) of the unbound nanomaterials were used as negative controls. The cells were next collected and suspended in 500 μl of the provided binding buffer. Cells were then treated with 5 μl Annexin-V-fluorescein isothiocyanate and 5 μl propidium iodide and incubated at room temperature in the dark for 15 min. Cells were analyzed using a BD FacsCalibur flow cytometer and FACS Diva software.

Nile Red Staining Assay

We chose to study the effect of our combined treatment on the accumulation of intracellular lipid droplets in MCF-7 and Panc-1 cell lines as lipids are stored in separate droplets in the cytosol of most eukaryotic cells and participate in different cellular mechanisms (Murphy and Vance, 1999; Zweytick *et al.*, 2000). Nile Red was selected for these experiments because it has been shown to be superior to other fluorescent dyes, such as rhodamines and nitrobenzoxadiazol, for the staining of intracellular lipids (Greenspan and Fowler, 1985; Greenspan *et al.*, 1985). Cells were stained with Nile Red (Sigma-Aldrich) to detect intracellular lipid droplets. Briefly, 1×10^3 cells were seeded on to eight-well chamber slides and incubated with GA (1 μg ml^{-1}) and GA + Gn (Gn = 10 μg ml^{-1}) for 48 h. Normal growth medium and Gn were also used as negative controls. Cells were then collected, fixed with 4% formaldehyde, rinsed three times with phosphate-buffered saline, incubated with Nile Red stain for 15 min, and visualized by fluorescence microscopy.

DNA Fragmentation Assay

DNA fragmentation induced by GA + Gn and GA + SWCNT in MCF-7 and Panc-1 cancer cells was assayed using the Quick Apoptotic DNA ladder Detection Kit (Biovision). Briefly, 1×10^6 cells were seeded in 35 mm dishes and incubated with GA (1 μg ml^{-1}), GA + Gn (Gn = 10 μg ml^{-1}) and GA + SWCNT (SWCNT = 10 μg ml^{-1}) for 48 h. Cells were then collected and assayed according to the manufacturer's instructions. The final DNA pellet

was dissolved in the provided suspension buffer, separated on 1.2% agarose containing 0.5 μg ml^{-1} ethidium bromide, and visualized by transillumination.

Statistical Analysis

All data are presented as mean ± SEM. The data were analyzed using two-way analysis of variance by Prism 5 software. $P < 0.05$ was considered statistically significant.

Results

Characterization of Nanomaterials and Initial Drug Loading on the Surface of Graphene and Single-Walled Carbon Nanotube

TEM measurements of the carbon nanomaterials indicated that the purchased SWCNT had a diameter of 1.5–2 nm, and the few-layer Gn structures had an average size of 100–200 nm (Fig. 1). GA was loaded onto the surface of Gn and SWCNT, and UV-Vis analysis of GA + Gn and GA + SWCNT showed a peak at 360 nm, which is the characteristic wavelength for the GA structure (Fig. 2). The amount of drug loaded was calculated by peak absorbance at 360 nm after subtracting the background of absorbance from Gn and SWCNT. We determined that, after vortexing, 98% of the free GA was bound to the Gn (GA–Gn = 0.98 : 10 μg ml^{-1}) and that 88% was bound to the SWCNT (GA–SWCNT = 0.88 : 10 μg ml^{-1}).

Concentration-Dependent Toxicity of Graphene and Single-Walled Carbon Nanotubes and Cellular Uptake

To determine which concentration of nanomaterials was most suitable for use in future experiments, the concentration-dependent cell membrane integrity assay (LDH) was used with both cell lines. Released LDH in the culture supernatants was analyzed by using a coupled enzymatic assay that generates the transformation of a reduced tetrazolium salt (INT) into a colored formazan product, which absorbs strongly in the spectral range of 490–520 nm. MCF-7 and Panc-1 cells were treated with increasing concentrations of Gn or SWCNT, and LDH release was measured after three time points up to 72 h (Fig. 3). Although there was a modest toxicity level at high concentrations from both nanomaterials in both cell lines, there was no significant toxicity measured at 10 μg ml^{-1}. Our results were in agreement with previous studies that have shown no toxicity at concentrations less than 20 μg ml^{-1} (Mahmood *et al*., 2013; Wang K *et al*., 2011). Therefore, 10 μg ml^{-1} was chosen as the maximum concentration to be used in our study, and each cell treatment presented here contained 10 μg ml^{-1} or less of nanomaterial.

Transmission Electron Microscopy Analysis of Cell Culture

To verify that both the SWCNT and Gn used as drug carriers were taken up by the cells, TEM was performed (Fig. 4). Micrographs of PANC-1 cells were taken after 24h of incubation with the nanomaterials. The micrographs indicated that the nanomaterials were taken-up through the cytoplasmic membrane.

Inhibition of MCF-7 and Panc-1 Cell Viability by Gambogic Acid, Gambogic Acid + Graphene and Gambogic Acid + Single-Walled Carbon Nanotube

To investigate whether the nanodelivery of GA increased the efficacy of GA treatment, MCF-7 and Panc-1 were treated with increasing concentrations of GA (0–1 μg ml^{-1}) at a constant Gn or SWCNT concentration (10 μg ml^{-1}). The IC_{50} values after 24, 48, and 72 h of incubation with free GA were determined (48 h data shown in Fig. 5). Treatment of Panc-1 cells resulted in IC_{50} values of 3.0, 1.9, and 1.2 μg ml^{-1} for the three time points, respectively. These numbers were slightly higher than those seen with MCF-7 (2.6, 1.7, and 1.4 μg ml^{-1}, respectively). GA bound to Gn and SWCNT showed significantly higher cytotoxicity (i.e., lower IC_{50} values) than GA treatment alone (Fig. 5). GA + Gn treatment was found to be slightly more effective than treatment with GA + SWCNT. IC_{50} values of 0.56 and 0.63 for MCF-7 and Panc-1, respectively, were seen for GA + Gn, while the cells treated with GA + SWCNT showed IC_{50} values of 0.64 and 0.68 μg ml^{-1} for MCF-7 and Panc-1 cells, respectively.

Induced Disruption of Mitochondrial Membrane Potential (ΔΨm) by Nanodelivered Gambogic Acid

The JC-1 staining method was used to monitor mitochondrial health. The mitochondrial membrane potential of MCF-7 and Panc-1 cells was detected after 24 h of treatment (Fig. 6). As mitochondria are considered one of the key organelles that control the energy supply of cells as well as the cellular apoptosis mechanism, any imbalance in the mitochondrial membrane potential, ΔΨm, causes membrane depolarization and induces a cascade of mitochondrion-dependent apoptotic signaling. Depolarization of mitochondrial membrane potential interrupts the dye's accumulation in the mitochondrial matrix, and, as a result, the dye is dispersed in the cytoplasm. In healthy cells, JC-1 aggregates and emits red fluorescence in mitochondria of high membrane potentials. Unhealthy cells lose their cross-membrane electrochemical gradient, causing JC-1 to dissociate into monomers and emit green fluorescence. The ratio of green to red fluorescence provides a dependable estimate of mitochondrial impairment. Fluorescent microscopic images of both cell lines treated with GA (1 μg ml^{-1}), GA + Gn (1 + 10 μg ml^{-1}), and GA + SWCNT (0.9 + 10 μg ml^{-1}) clearly show the presence of a high level of JC-1 monomer in the cytoplasm. This effect was much more pronounced in MCF-7 than in Panc-1 cells. Panc-1 cells showed a marked increase in the number of green cells when treated with GA + Gn or GA + SWCNT, and MCF-7 cells showed a significant reduction in the number of cells visible after treatment with the nanodelivered GA.

Cellular Death Study Performed by Flow Cytometry

Flow cytometry studies were performed in order to quantify the percentages of apoptotic and necrotic cells after GA nanodelivery (Fig. 7). The percentage of dead cells after treatment with increasing concentrations of GA + Gn and GA + SWCNT for 24 and 48 h was significantly higher than after treatment with GA alone. In Panc-1 cells, the number of dead cells after nanodelivery was only significantly higher at the highest concentrations. In MCF-7 cells, the effects were seen at lower concentrations with GA + SWCNT showing increased toxicity starting at ~ 0.65 mg ml^{-1} ($P < 0.001$), and with GA + Gn showing

significantly higher numbers of dead cells at all three concentrations ($P < 0.001$). Unbound nanomaterials (Gn and SWCNT) had a negligible cytotoxic effect on MCF-7 and Panc-1 cells with > 90% of cells remaining viable even after 48 h. These data are in agreement with the LDH release data presented in Fig. 3. Taken together, these results demonstrate the increased cytotoxicity of GA + Gn and GA + SWCNT as compared to GA alone.

Intracellular Lipid Droplet Detection

The effect of GA, alone and delivered by Gn, on the intracellular lipid content of MCF-7 and Panc-1 cells was assessed by staining cells with Nile Red dye after 48 h incubation with GA, Gn, and GA + Gn (Fig. 8). The images visibly prove that the lipid droplets were affected more by GA when delivered as GA + Gn than by GA alone. Lipid droplets serve as lipid storage for energy generation, membrane synthesis, and protein degradation (Walther and Farese, 2012). Therefore, the diminished levels of lipids found after treatment with GA + Gn revealed that Gn delivery improved the efficacy of GA in MCF-7 and Panc-1 cells.

DNA Fragmentation

DNA fragmentation induced by GA + Gn and GA + SWCNT in MCF-7 and Panc-1 cancer cells was assessed (Fig. 9). Nuclear DNA fragmentation is considered a hallmark of apoptosis. DNA that has degraded into nucleic acid is considered an indicator of apoptotic cell death and occurs in response to different apoptotic stimuli in a broad range of cell types (Rahman *et al.*, 2013). Generally, DNA fragmentation into regions to produce 180–185 base pairs gives the distinguishing ladder appearance in agarose gel electrophoresis (Ioannou and Chen, 1996). For both MCF-7 and Panc-1 cells, nanodelivered GA induced more DNA fragmentation than GA, alone, with GA + Gn being the most effective.

Discussion

The possible use of GA for the treatment of cancer is a growing area of study, and, while this naturally derived drug has shown promise, its use is limited by its poor solubility (He *et al.*, 2012) and inadequate oral bioavailability (Zhang *et al.*, 2013). One of bio-nanotechnology's many contributions to the field of drug delivery is the ability to improve the water solubility of drugs, enhance their cellular uptake, and increase formulation stability and shelf life (De Jong and Borm, 2008). This study reports the first use of carbon-based nanomaterials, Gn and SWCNT, for the efficient delivery of GA to cancer cells *in vitro*.

As with all medical developments, possible undesirable side-effects remain one of the major obstacles to using Gn and SWCNT as medicinal delivery agents. A tremendous amount of research has been dedicated to the study of the toxicity of these materials, but, to date, no significant cytotoxicity has been reported for Gn when delivered at low concentrations. Low concentrations of Gn oxide (less than 20 μg ml^{-1}) did not demonstrate any toxic effect when delivered to various cell lines (Chang *et al.*, 2011; Lee *et al.*, 2012; Mahmood *et al.*, 2013; Wang K *et al.*, 2011). Similarly, Gn oxide did not show any obvious toxicity when delivered *in vivo* to mice in concentrations of 0.1 mg or 0.25 mg (Wang K *et al.*, 2011). All of the nanomaterials used in this study were functionalized with carboxyl groups to ensure greater

solubility and to prevent their agglomeration, which may interfere with their cellular internalization. Our results demonstrated that approximately 94–95% of the cells survived when treated with 10 μg ml^{-1} SWCNT and Gn and incubated for up to 48 h.

The effectiveness of this method of delivery is assessed by comparing cancer cell survival and the lipid contents of cells treated with GA alone and with GA + Gn and GA + SWCNT. Gn and SWCNT were able to lower the doses of the drug needed to inhibit the cellular proliferation by 50% when delivered to MCF-7 and Panc-1 cell lines. More work will be conducted to improve this approach further using molecular targeting techniques, which will allow more precisely targeted delivery of these compounds to specific cancers and lead to even better outcomes, as well as a reduction in systemic toxicity.

There is increasing evidence that cancer cells show specific alterations in lipid metabolism. Lipids play an important role in cellular signaling, functioning both as hormones and secondary messengers. In contrast to normal cells, cancer cells rely heavily on anaerobic glycolysis for energy production (Vander Heiden *et al.*, 2009). Specifically, cancer cells have the capacity to synthesize their own supply of biologically active compounds of predominantly lipid origin, such as phosphatidyl serine and other phospholipids, as well as estrogens, androgens, farnesyl, oxysteroids, and fatty acids (Vander Heiden *et al*., 2009). Therefore, Nile Red staining allowed us to evaluate the changes in lipid levels before and after treatment with GA, as well as to compare levels between cells treated with GA alone and with nanodelivery by either Gn or SWCNT. These experiments confirmed that the dramatic changes in the lipid content of cancer cells were not caused by the Gn, itself, but that the Gn delivery enhanced the cytotoxic effects of GA. This is a novel approach and can be used for the evaluation of the effect of nanodelivery of other anticancer molecules, such as drugs and DNA.

The method of action for GA as an anticancer drug is a growing area of study, and many different mechanisms have been suggested. At the present, we can only speculate about how nanodelivery may affect the mechanism of action of GA. Figure 10 illustrates our proposed method of GA + Gn and GA + SWCNT entry into the cells and the intracellular targets investigated here. The literature shows that GA can generate apoptosis through upregulation of multiple proteins, including p53 (tumor protein 53) (Gu *et al.*, 2008), Bcl-2 (B-cell lymphoma 2) (Kasibhatla *et al.*, 2005), TtR (transferrin receptor) (Kasibhatla *et al.*, 2005), and hTERT (human telomerase reverse transcriptase) (Yu *et al.*, 2006). It has also been shown to generate apoptosis through stimulating the expression of caspase 9 and 3 (Wang C *et al*., 2011) and to inhibit tyrosine kinase receptor-mediated angiogenesis (Wang and Chen, 2012). Some or all of these pathways may be involved in producing the cytotoxic effects of GA + Gn complexes; however, new mechanisms could also be involved. It is possible that nanodelivery of GA to cancer cells not only increases cellular concentrations due to improved solubility, but may also direct this compound to different molecular targets within the cells, exposing new enzymes and receptors to the effects of this drug. For example, we have unpublished data suggesting that GA acts as a partial agonist at cannabinoid receptors. In normal cells, cannabinoid receptors are localized at the plasma membrane; however, in both breast and pancreatic cancer cells, CB1 and CB2 are also translocated into the perinuclear area within the cell (Carracedo *et al*., 2006). GA + Gn may deliver GA into the

cells in such a way that increases the effectiveness of GA as a CB2 antagonist. Experiments are in progress to investigate this option.

Conclusions

We present here data supporting the hypothesis that Gn and SWCNT can serve as an effective nontoxic mode of delivery of GA into cancer cells. These nanomaterials were able to induce significant improvement in GA chemotherapeutic efficiency after endocytosis. We postulate that this increase in anticancer activity may be due in part to increasing its water solubility and cellular uptake and possibly by directing this compound to different molecular targets within the cell. This analysis of GA + Gn and GA + SWCNT represents a first step toward assessing their effectiveness in more complex, targeted nanodelivery systems. These *in vitro* studies may then lead to more translational work to assess their potential applications in the fields of pharmacology and medicine.

Acknowledgments

This work was funded by grants from the Department of Defense (X81XWH-11-1-0795) to A.S.B. and A.R.-P., and from the Arkansas Breast Cancer Research Program/University of Arkansas for Medical Sciences Translational Research Institute Clinical Translational Science Award (UL1TR000039) to A.R.-P.

References

Biris AR, Mahmood M, Lazar MD, Dervishi E, Watanabe F, Mustafa T, Baciut G, Baciut M, Bran S, Ali S, Biris AS. Novel multicomponent and biocompatible nanocomposite materials based on few-layer graphenes synthesized on a gold/hydroxyapatite catalytic system with applications in bone regeneration. J Phys Chem C. 2011; 115:18967–18976.

Carracedo A, Gironella M, Lorente M, Garcia S, Guzman M, Velasco G, Iovanna JL. Cannabinoids induce apoptosis of pancreatic tumor cells via endoplasmic reticulum stress-related genes. Cancer Res. 2006; 66:6748–6755. [PubMed: 16818650]

Chang Y, Yang ST, Liu JH, Dong E, Wang Y, Cao A, Liu Y, Wang H. In vitro toxicity evaluation of graphene oxide on A549 cells. Toxicol Lett. 2011; 200:201–210. [PubMed: 21130147]

Chantarasriwong O, Batova A, Chavasiri W, Theodorakis EA. Chemistry and biology of the caged Garcinia xanthones. Chemistry. 2010; 16:9944–9962. [PubMed: 20648491]

Chen B, Liang Y, Wu W, Cheng J, Xia G, Gao F, Ding J, Gao C, Shao Z, Li G, Chen W, Xu W, Sun X, Liu L, Li X, Wang X. Synergistic effect of magnetic nanoparticles of Fe(3)O(4) with gambogic acid on apoptosis of K562 leukemia cells. Int J Nanomed. 2009; 4:251–259.

De Jong WH, Borm PJ. Drug delivery and nanoparticles: applications and hazards. Int J Nanomed. 2008; 3:133–149.

Dervishi E, Biris A, Watanabe F, Umwungeri J, Mustafa T, Driver J, Biris A. Few-layer nano-graphene structures with large surface areas synthesized on a multifunctional Fe:Mo:MgO catalyst system. J Mater Sci. 2012; 47:1910–1919.

Efferth T, Li PCH, Konkimalla VSB, Kaina B. From traditional Chinese medicine to rational cancer therapy. Trends Mol Med. 2007; 13:353–361. [PubMed: 17644431]

Fang L, Chen B, Liu S, Wang R, Hu S, Xia G, Tian Y, Cai X. Synergistic effect of a combination of nanoparticulate Fe3O4 and gambogic acid on phosphatidylinositol 3-kinase/Akt/Bad pathway of LOVO cells. Int J Nanomed. 2012; 7:4109–4118.

Geim AK, Novoselov KS. The rise of graphene. Nat Mater. 2007; 6:183–191. [PubMed: 17330084]

Greenspan P, Fowler SD. Spectrofluorometric studies of the lipid probe, nile red. J Lipid Res. 1985; 26:781–789. [PubMed: 4031658]

Greenspan P, Mayer EP, Fowler SD. Nile red: a selective fluorescent stain for intracellular lipid droplets. J Cell Biol. 1985; 100:965–973. [PubMed: 3972906]

Gu H, Wang X, Rao S, Wang J, Zhao J, Ren FL, Mu R, Yang Y, Qi Q, Liu W, Lu N, Ling H, You Q, Guo Q. Gambogic acid mediates apoptosis as a p53 inducer through down-regulation of mdm2 in wild-type p53-expressing cancer cells. Mol Cancer Ther. 2008; 7:3298–3305. [PubMed: 18852133]

Guo QL, You QD, Wu ZQ, Yuan ST, Zhao L. General gambogic acids inhibited growth of human hepatoma SMMC-7721 cells in vitro and in nude mice. Acta Pharmacol Sin. 2004; 25:769–774. [PubMed: 15169630]

He L, Ling Y, Fu L, Yin D, Wang X, Zhang Y. Synthesis and biological evaluation of novel derivatives of gambogic acid as anti-hepatocellular carcinoma agents. Bioorg Med Chem Lett. 2012; 22:289–292. [PubMed: 22153338]

Iijima S. Helical microtubules of graphitic carbon. Nature. 1991; 354:56–58.

Ioannou YA, Chen FW. Quantitation of DNA fragmentation in apoptosis. Nucleic Acids Res. 1996; 24:992–993. [PubMed: 8600475]

Jemal A, Bray F, Center MM, Ferlay J, Ward E, Forman D. Global cancer statistics. CA Cancer J Clin. 2011; 61:69–90. [PubMed: 21296855]

Karmakar A, Bratton SM, Dervishi E, Ghosh A, Mahmood M, Xu Y, Saeed LM, Mustafa T, Casciano D, Radominska-Pandya A, Biris AS. Ethylenediamine functionalized-single-walled nanotube (f-SWNT)-assisted in vitro delivery of the oncogene suppressor p53 gene to breast cancer MCF-7 cells. Int J Nanomed. 2011; 6:1045–1055.

Kasibhatla S, Jessen KA, Maliartchouk S, Wang JY, English NM, Drewe J, Qiu L, Archer SP, Ponce AE, Sirisoma N, Jiang S, Zhang HZ, Gehlsen KR, Cai SX, Green DR, Tseng B. A role for transferrin receptor in triggering apoptosis when targeted with gambogic acid. Proc Natl Acad Sci U S A. 2005; 102:12095–12100. [PubMed: 16103367]

Kim TH, Kim HS. Effect of acid-treated carbon nanotube and amine-terminated polydimethylsiloxane on the rheological properties of polydimethylsiloxane/carbon nanotube composite system. Korea-Aust Rheol J. 2010; 22:205–210.

Lee J, Shin Y, Jin O, Lee E, Han D-W, Kang S, Hong S, Ahn J, Kim S. Cytotoxicity evaluations of pristine graphene and carbon nanotubes in fibroblastic cells. J Korean Phys Soc. 2012; 61:873–877.

Liang YQ, Chen BA, Wu WW, Gao F, Xia GH, Shao ZY, Cheng J, Ding JH, Gao C, Li GH, Chen WJ, Chen NN, Xu WL, Sun XC, Liu LJ, Li XM, Wang XM. Effects of magnetic nanoparticle of Fe3O4 on apoptosis induced by Gambogic acid in U937 leukemia cells. Zhongguo Shi Yan Xue Ye Xue Za Zhi. 2010; 18:67–73. [PubMed: 20137121]

Liu Z, Robinson JT, Sun X, Dai H. PEGylated nanographene oxide for delivery of water-insoluble cancer drugs. J Am Chem Soc. 2008; 130:10876–10877. [PubMed: 18661992]

Liu Z, Robinson JT, Tabakman SM, Yang K, Dai H. Carbon materials for drug delivery and cancer therapy. Mater Today. 2011; 14:316–323.

Mahmood M, Karmakar A, Fejleh A, Mocan T, Iancu C, Mocan L, Iancu DT, Xu Y, Dervishi E, Li Z, Biris AR, Agarwal R, Ali N, Galanzha EI, Biris AS, Zharov VP. Synergistic enhancement of cancer therapy using a combination of carbon nanotubes and anti-tumor drug. Nanomedicine (Lond). 2009; 4:883–893. [PubMed: 19958225]

Mahmood M, Casciano D, Xu Y, Biris AS. Engineered nanostructural materials for application in cancer biology and medicine. J Appl Toxicol. 2012; 32:10–19. [PubMed: 21882206]

Mahmood M, Xu Y, Dantuluri V, Mustafa T, Zhang Y, Karmakar A, Casciano D, Ali S, Biris A. Carbon nanotubes enhance the internalization of drugs by cancer cells and decrease their chemoresistance to cytostatics. Nanotechnology. 2013; 24:045102. [PubMed: 23291321]

Murphy DJ, Vance J. Mechanisms of lipid-body formation. Trends Biochem Sci. 1999; 24:109–115. [PubMed: 10203758]

Novoselov KS, Geim AK, Morozov SV, Jiang D, Zhang Y, Dubonos SV, Grigorieva IV, Firsov AA. Electric field effect in atomically thin carbon films. Science. 2004; 306:666–669. [PubMed: 15499015]

Qi Q, Lu N, Wang XT, Gu HY, Yang Y, Liu W, Li C, You QD, Guo QL. Anti-invasive effect of gambogic acid in MDA-MB-231 human breast carcinoma cells. Biochem Cell Biol. 2008; 86:386–395. [PubMed: 18923540]

Qu G, Zhu X, Zhang C, Ping Q. Modified chitosan derivative micelle system for natural anti-tumor product gambogic acid delivery. Drug Deliv. 2009; 16:363–370. [PubMed: 19575591]

Rahman MA, Kim NH, Huh SO. Cytotoxic effect of gambogic acid on SH-SY5Y neuroblastoma cells is mediated by intrinsic caspase-dependent signaling pathway. Mol Cell Biochem. 2013; 377:187–196. [PubMed: 23404459]

Safioleas MC, Moulakakis KG. Pancreatic cancer today. Hepatogastroenterology. 2004; 51:862–868. [PubMed: 15143935]

Saxena V, Hussain MD. Poloxamer 407/TPGS mixed micelles for delivery of gambogic acid to breast and multidrug-resistant cancer. Int J Nanomed. 2012; 7:713–721.

Siegel R, Naishadham D, Jemal A. Cancer statistics. CA Cancer J Clin. 2013; 63:11–30. [PubMed: 23335087]

Sun X, Liu Z, Welsher K, Robinson J, Goodwin A, Zaric S, Dai H. Nano-graphene oxide for cellular imaging and drug delivery. Nano Res. 2008; 1:203–212. [PubMed: 20216934]

Sundar S, Prajapati VK. Drug targeting to infectious diseases by nanoparticles surface functionalized with special biomolecules. Curr Med Chem. 2012; 19:3196–3202. [PubMed: 22612703]

Tod J, Jenei V, Thomas G, Fine D. Tumor-stromal interactions in pancreatic cancer. Pancreatology. 2013; 13:1–7. [PubMed: 23395563]

Vander Heiden MG, Cantley LC, Thompson CB. Understanding the Warburg effect: the metabolic requirements of cell proliferation. Science. 2009; 324:1029–1033. [PubMed: 19460998]

Walther TC, Farese RV Jr. Lipid droplets and cellular lipid metabolism. Annu Rev Biochem. 2012; 81:687–714. [PubMed: 22524315]

Wang C, Zhang H, Chen B, Yin H, Wang W. Study of the enhanced anticancer efficacy of gambogic acid on Capan-1 pancreatic cancer cells when mediated via magnetic Fe_3O_4 nanoparticles. Int J Nanomed. 2011; 6:1929–1935.

Wang C, Zhang H, Chen Y, Shi F, Chen B. Gambogic acid-loaded magnetic Fe_3O_4 nanoparticles inhibit Panc-1 pancreatic cancer cell proliferation and migration by inactivating transcription factor ETS1. Int J Nanomed. 2012; 7:781–787.

Wang K, Ruan J, Song H, Zhang J, Wo Y, Guo S, Cui D. Biocompatibility of graphene oxide. Nanoscale Res Lett. 2011; 6:1–8.

Wang LL, Li ZL, Song DD, Sun L, Pei YH, Jing YK, Hua HM. Two novel triterpenoids with antiproliferative and apoptotic activities in human leukemia cells isolated from the resin of Garcinia hanburyi. Planta Med. 2008; 74:1735–1740. [PubMed: 18781544]

Wang X, Chen W. Gambogic acid is a novel anti-cancer agent that inhibits cell proliferation, angiogenesis and metastasis. Anticancer Agents Med Chem. 2012; 12:994–1000. [PubMed: 22339063]

Wu ZQ, Guo QL, You QD, Zhao L, Gu HY. Gambogic acid inhibits proliferation of human lung carcinoma SPC-A1 cells in vivo and in vitro and represses telomerase activity and telomerase reverse transcriptase mRNA expression in the cells. Biol Pharm Bull. 2004; 27:1769–1774. [PubMed: 15516720]

Xu Y, Karmakar A, Heberlein WE, Mustafa T, Biris AR, Biris AS. Multifunctional magnetic nanoparticles for synergistic enhancement of cancer treatment by combinatorial radio frequency thermolysis and drug delivery. Adv Healthc Mater. 2012; 1:493–501. [PubMed: 23184783]

Yu F, He C, Waddad AY, Munyendo WL, Lv H, Zhou J, Zhang Q. N-octyl-N-arginine-chitosan (OACS) micelles for gambogic acid oral delivery: preparation, characterization and its study on in situ intestinal perfusion. Drug Dev Ind Pharm. 201310.3109/03639045.2013.786723

Yu J, Guo QL, You QD, Lin SS, Li Z, Gu HY, Zhang HW, Tan Z, Wang X. Repression of telomerase reverse transcriptase mRNA and hTERT promoter by gambogic acid in human gastric carcinoma cells. Cancer Chemother Pharmacol. 2006; 58:434–443. [PubMed: 16470410]

Zhang L, Xia J, Zhao Q, Liu L, Zhang Z. Functional graphene oxide as a nanocarrier for controlled loading and targeted delivery of mixed anticancer drugs. Small. 2010; 6:537–544. [PubMed: 20033930]

Zhang X, Li X, Sun H, Wang X, Zhao L, Gao Y, Liu X, Zhang S, Wang Y, Yang Y, Zeng S, Guo Q, You Q. Garcinia xanthones as orally active antitumor agents. J Med Chem. 2013; 56:276–292. [PubMed: 23167526]

Zhang Y, Ali SF, Dervishi E, Xu Y, Li Z, Casciano D, Biris AS. Cytotoxicity effects of graphene and single-wall carbon nanotubes in neural phaeochromocytoma-derived PC12 cells. ACS Nano. 2010; 4:3181–3186. [PubMed: 20481456]

Zhang Y, Nayak TR, Hong H, Cai W. Graphene: a versatile nanoplatform for biomedical applications. Nanoscale. 2012; 4:3833–3842. [PubMed: 22653227]

Zhu X, Zhang C, Wu X, Tang X, Ping Q. Preparation, physical properties, and stability of gambogic acid-loaded micelles based on chitosan derivatives. Drug Dev Ind Pharm. 2008; 34:2–9. [PubMed: 18214750]

Zweytick D, Athenstaedt K, Daum G. Intracellular lipid particles of eukaryotic cells. Biochim Biophys Acta. 2000; 1469:101–120. [PubMed: 10998572]

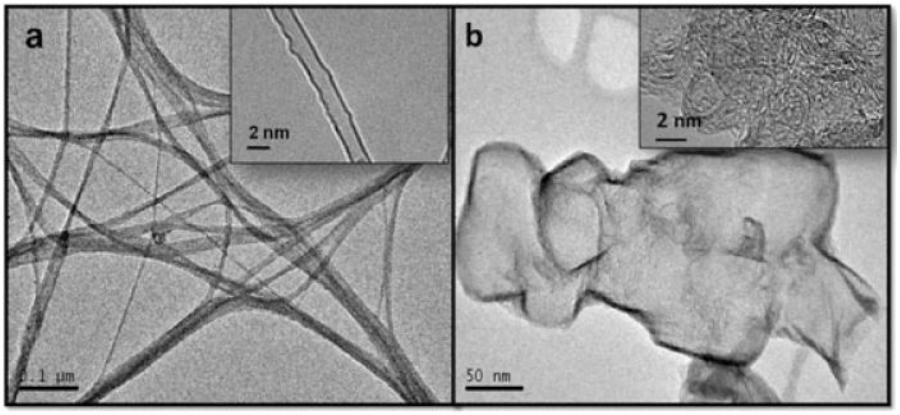

Figure 1.

Representative transmission electron microscopy micrographs of the graphene and single-walled carbon nanotube nanomaterials used in this study. (a) Transmission electron microscopy micrographs of the (a) crystalline carboxylated single-walled carbon nanotube, and (b) carboxylated nano-graphene structures synthesized on the Fe:Mo:MgO bimetallic system. Each inset shows the same material at a higher resolution.

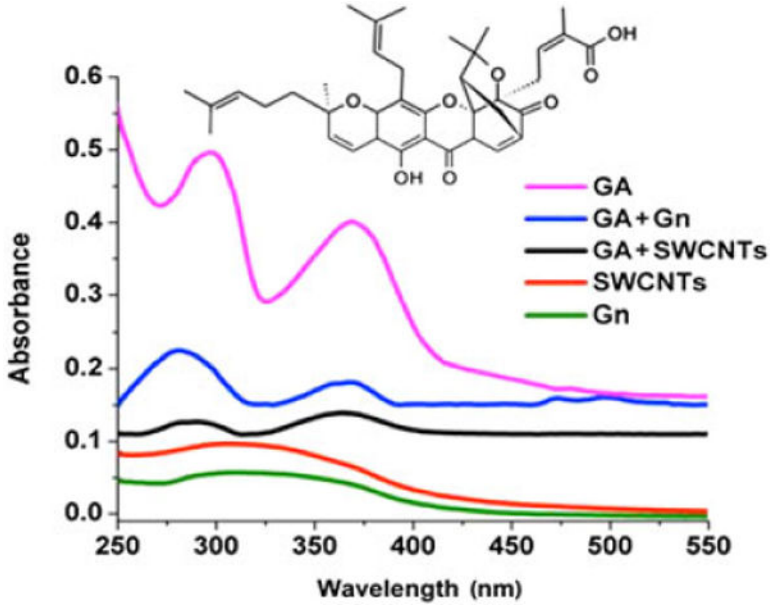

Figure 2.

Ultraviolet visible spectra of GA, Gn, SWCNT, GA + Gn, and GA + SWCNT. Ultraviolet visible spectra for free GA, Gn, and SWCNTs were compared to that of GA + Gn and GA + SWCNT to determine the amount of GA loaded onto the surface of these nanomaterials. The chemical structure of GA is illustrated. GA, gambogic acid; Gn, graphene; SWCNT, single-walled carbon nanotube.

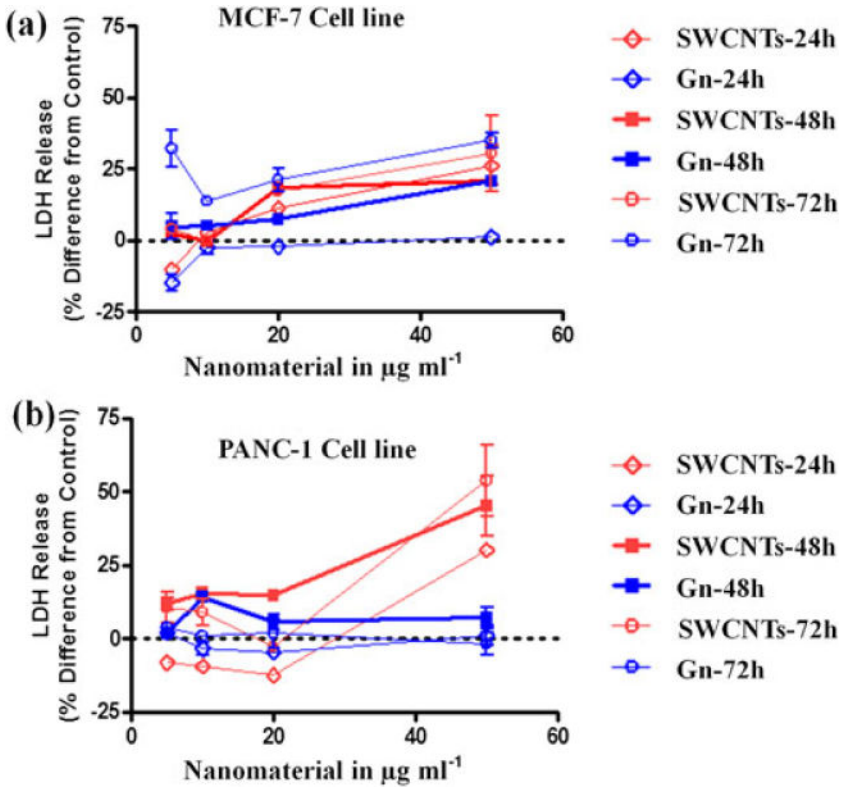

Figure 3.

LDH enzyme release from MCF-7 and Panc-1 cells treated with Gn and SWCNT. Cells were treated with increasing concentrations of nanomaterials (1–50 µg ml^{-1}) and concentration-dependent toxicity of these materials after 24, 48, and 72 h of exposure was determined based on the release of LDH from the cells. Data were collected from three independent experiments performed in duplicate (n = 6) and presented as mean ± SEM. Gn, graphene; LDH, lactate dehydrogenase; SWCNT, single-walled carbon nanotube.

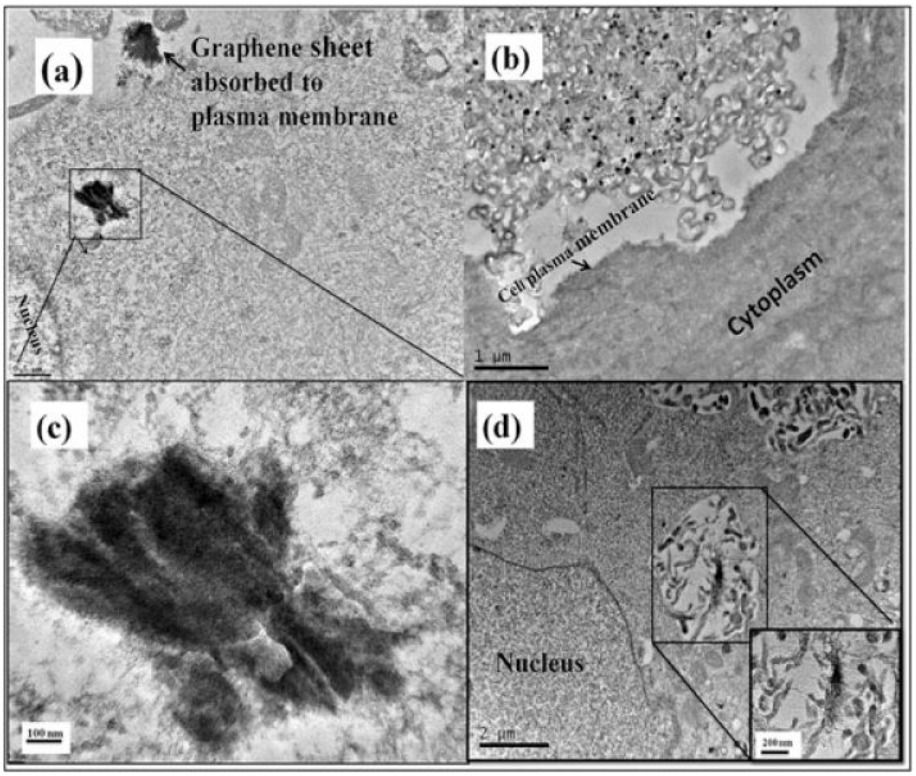

Figure 4.

Representative photomicrographs of transmission electron microscopy of PANC-1 cells incubated with 10 μg ml^{-1} of graphene (a–c) and single-walled carbon nanotubes (d). The cells were incubated for 24 h.

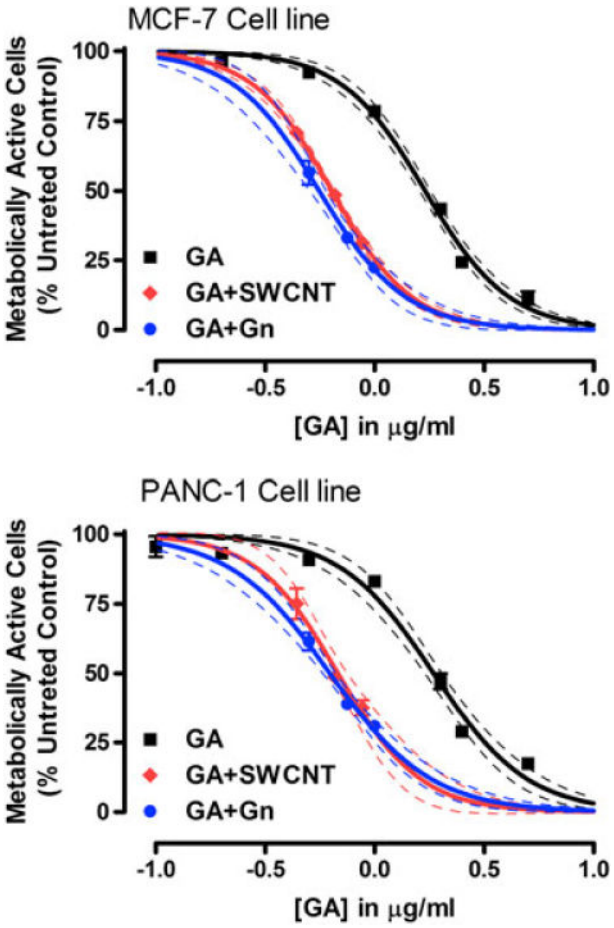

Figure 5.

WST-1 metabolic activity assay of MCF-7 and Panc-1 cells. Cells treated with GA, GA + Gn, and GA + SWCNT and assayed for cell viability using the WST-1 metabolic activity assay. All data are shown as the mean ± SEM and were obtained from three independent experiments performed in duplicate (n = 6). Generated data were fit to the Four Parameter Logistics Equation using Prism 5 software (GraphPad), and the curves were interpolated (and extrapolated) based on this equation and the understanding that the curve, which was normalized to the untreated controls, would have a maximum of 100% and a minimum of 0% viability or total cell death. 95% confidence limits are shown. GA, gambogic acid; Gn, graphene; SWCNT, single-walled carbon nanotube.

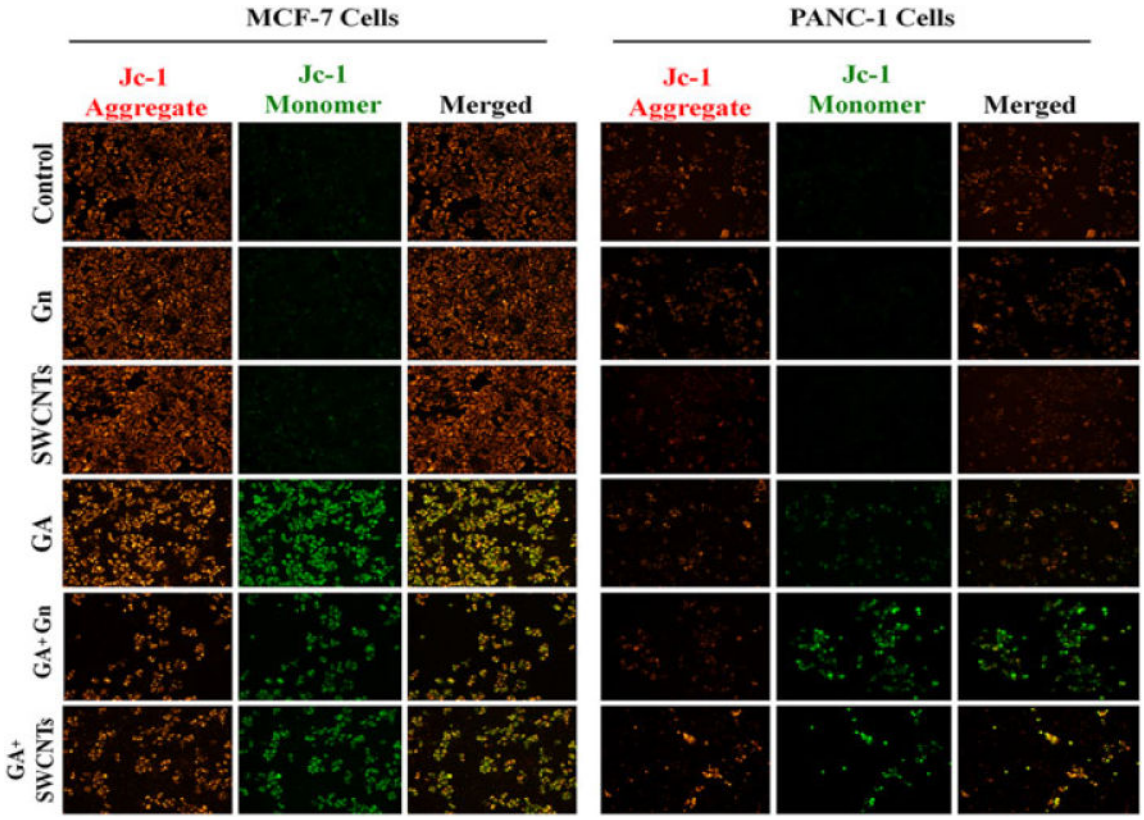

Figure 6.

Representative fluorescent microscopy images of JC-1 staining of MCF-7 and Panc-1 cells treated with GA, GA + Gn, and GA + SWCNT. MCF-7 and Panc-1 cells were incubated with GA (1 μg ml^{-1}), Gn (10 μg ml^{-1}), SWCNT (10 μg ml^{-1}), GA + Gn (1 + 10 μg ml^{-1}), and GA + SWCNT (0.9 + 10 μg ml^{-1}) for 24 h. The healthy mitochondria appear red (JC-1 aggregate) compared with the green J-monomer form found in the cytoplasm of cells with low $\Delta\psi m$. The data were obtained from three independent experiments (n = 3). GA, gambogic acid; Gn, graphene; SWCNT, single-walled carbon nanotube.

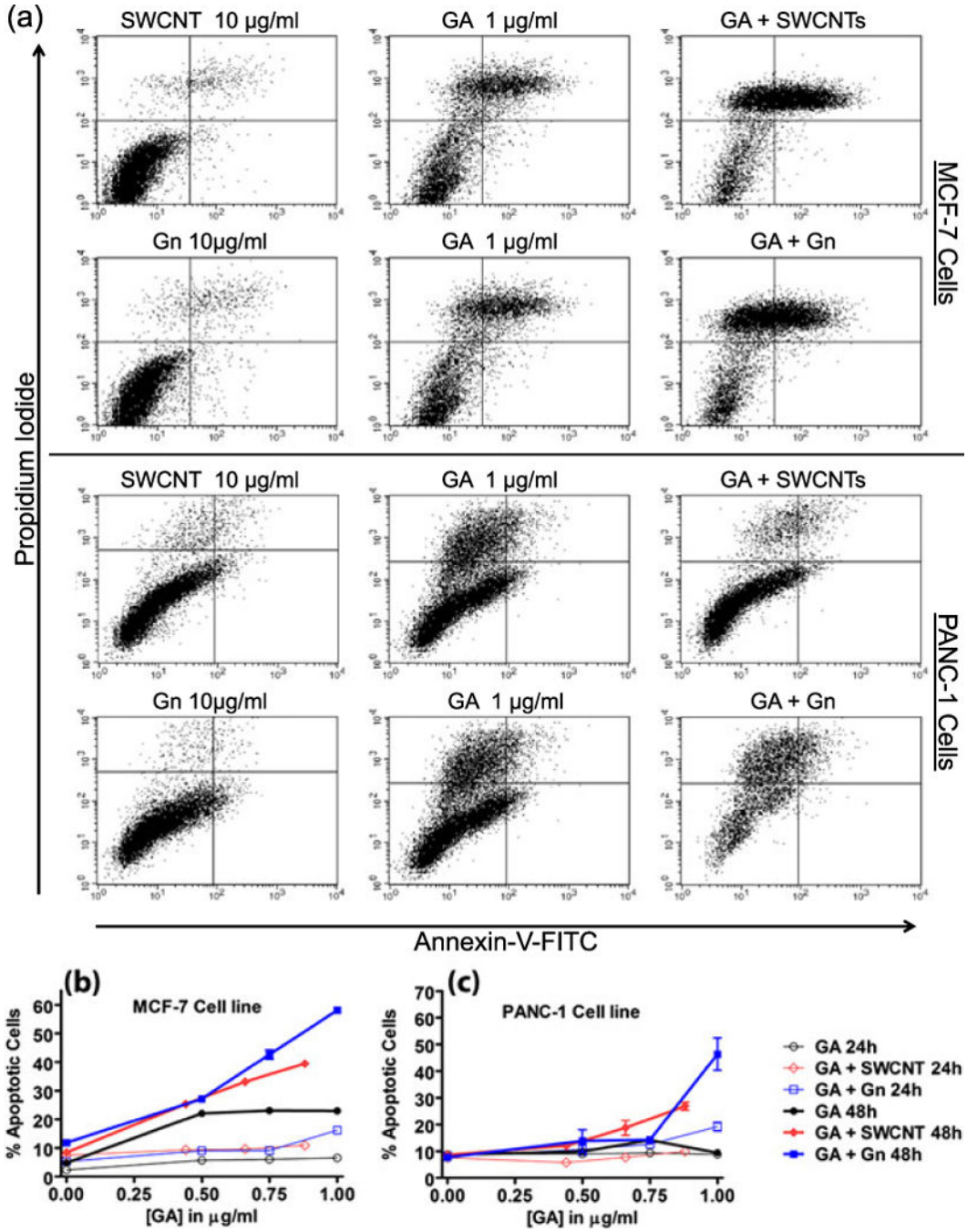

Figure 7.

Flow cytometry analysis of MCF-7 and Panc-1 cells treated with GA, GA + Gn and GA + SWCNT and stained with annexin-V/propidium iodide. (a) Representative histograms of flow cytometric analysis of the two cell lines after treatment with GA (1 µg ml^{-1}), Gn (10 µg ml^{-1}), SWCNT (10 µg ml^{-1}), GA + Gn (1 + 10 µg ml^{-1}), and GA + SWCNT (0.9 + 10 µg ml^{-1}) for 24 h. (b) The percentage of apoptotic MCF-7 and (c) Panc-1 cells after exposure to increasing concentrations of GA (0–1 µg ml^{-1}) at a constant Gn or SWCNT concentration

(10 μg ml^{-1}) for 24 and 48 h. FITC, fluorescein isothiocyanate; GA, gambogic acid; Gn, graphene; SWCNT, single-walled carbon nanotube.

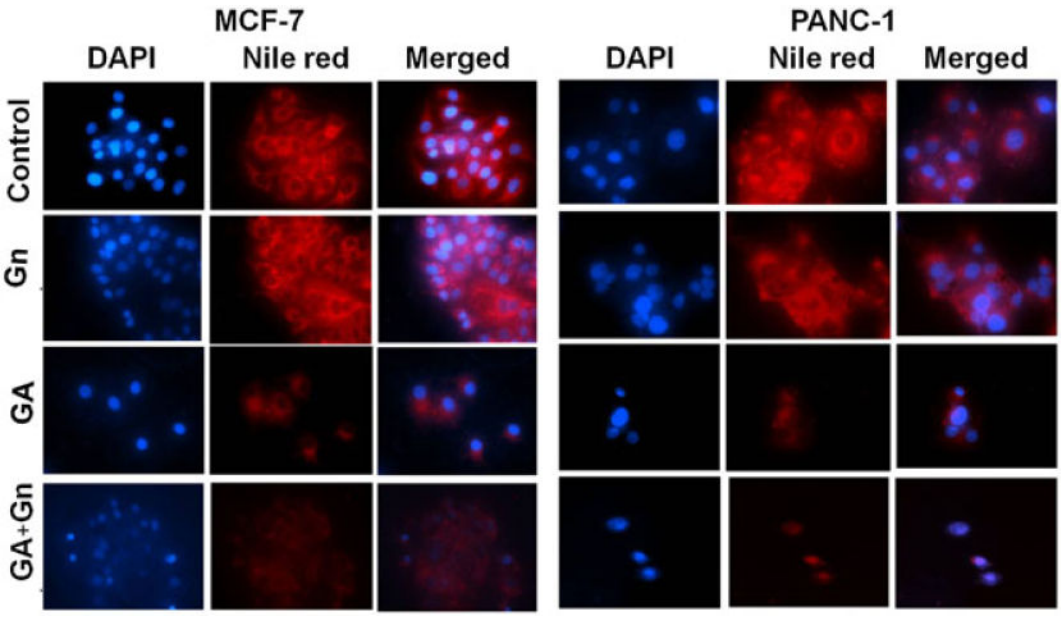

Figure 8.

Representative fluorescence microscopy images of MCF-7 and Panc-1 cells treated with GA, GA + Gn and stained with DAPI and Nile Red. MCF-7 and Panc-1 cells were incubated with GA (1 μg ml^{-1}), Gn (10 μg ml^{-1}), and GA + Gn (1 + 10 μg ml^{-1}) for 48 h. DAPI-stained nuclei appear blue, and Nile Red-stained lipids appear red. Data were obtained from three independent experiments (n = 3). GA, gambogic acid; Gn, graphene.

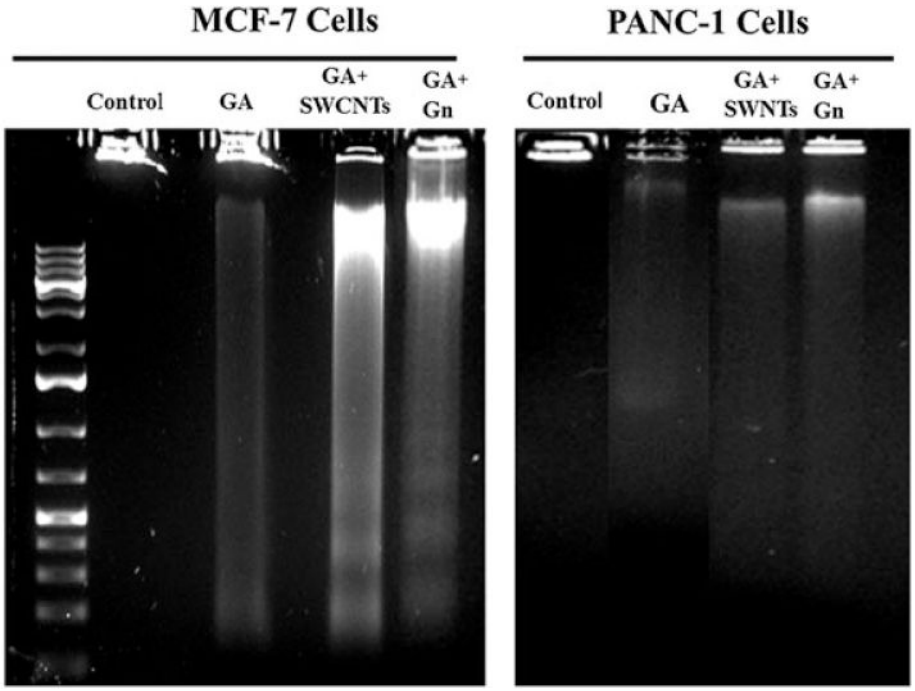

Figure 9.

DNA fragmentation in MCF-7 and Panc-1 cells treated with GA, GA + Gn and GA + SWCNT. MCF-7 and Panc-1 cells were incubated with GA (1 μg ml^{-1}), GA + SWCNT (0.9 + 10 μg/ml), and GA + Gn (1 + 10 μg ml^{-1}) for 48 h, after which DNA was collected, run on an ethidium bromide-stained agarose gel, and visualized by ultraviolet transillumination. GA, gambogic acid; Gn, graphene; SWCNT, single-walled carbon nanotube.

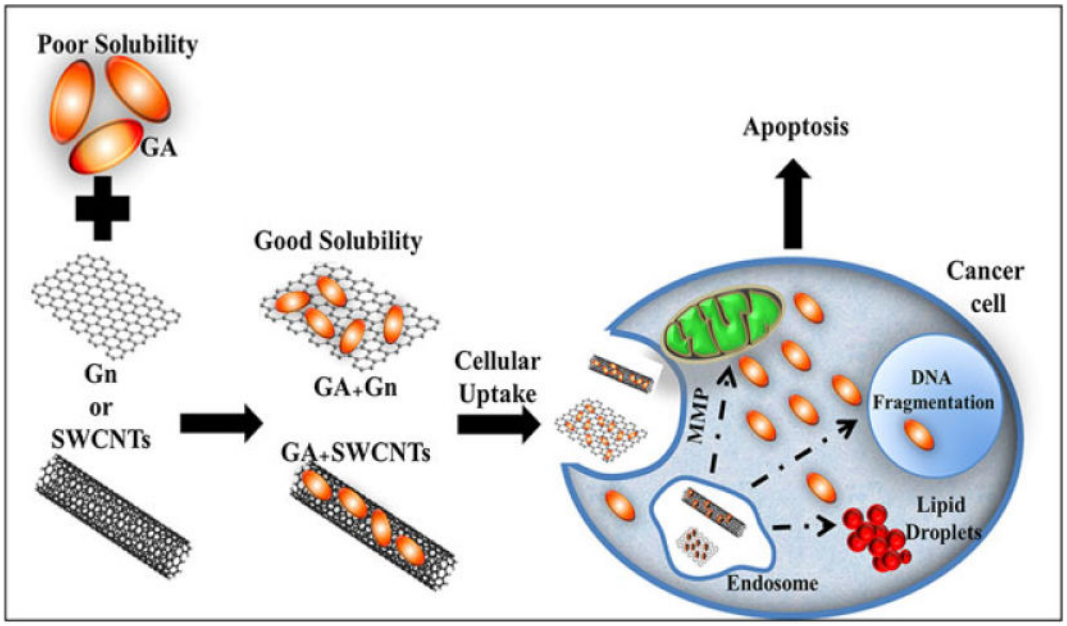

Figure 10.

Proposed method of cellular uptake and intracellular targets for GA + Gn, and GA + SWCNT. GA, gambogic acid; Gn, graphene; MMP, mitochondrial membrane potential; SWCNT, single-walled carbon nanotube.